The Journal of Immunology

# NFAT1 and JunB Cooperatively Regulate *IL-31* Gene Expression in CD4$^+$ T Cells in Health and Disease



Ji Sun Hwang, Gi-Cheon Kim, EunBee Park, Jung-Eun Kim, Chang-Suk Chae, Won Hwang, Changhon Lee, Sung-Min Hwang, Hui Sun Wang, Chang-Duk Jun, Dipayan Rudra and Sin-Hyeog Im

*J Immunol* 2015; 194:1963-1974; Prepublished online 16 January 2015;
doi: 10.4049/jimmunol.1401862
http://www.jimmunol.org/content/194/4/1963



*The Journal of Immunology* is published twice each month by
The American Association of Immunologists, Inc.,
1451 Rockville Pike, Suite 650, Rockville, MD 20852

Print ISSN: 0022-1767 Online ISSN: 1550-6606.

# NFAT1 and JunB Cooperatively Regulate *IL-31* Gene Expression in CD4$^+$ T Cells in Health and Disease

**Ji Sun Hwang,* Gi-Cheon Kim,*,† EunBee Park,* Jung-Eun Kim,*,† Chang-Suk Chae,* Won Hwang,*,† Changhon Lee,*,‡ Sung-Min Hwang,*,‡ Hui Sun Wang,§ Chang-Duk Jun,† Dipayan Rudra,* and Sin-Hyeog Im*,‡**

**IL-31 is a key mediator of itching in atopic dermatitis (AD) and is preferentially produced by activated CD4$^+$ T cells and Th2 cells. Although pathophysiological functions of IL-31 have been suggested in diverse immune disorders, the molecular events underlying *IL-31* gene regulation are still unclear. In this study we identified the transcription start site and functional promoter involved in *IL-31* gene regulation in mouse CD4$^+$ T cells. TCR stimulation–dependent IL-31 expression was found to be closely linked with in vivo binding of NFAT1 and JunB to the *IL-31* promoter. Although NFAT1 alone enhanced *IL-31* promoter activity, it was further enhanced in the presence of JunB. Conversely, knockdown of either NFAT1 or JunB resulted in reduced *IL-31* expression. NFAT1-deficient CD4$^+$ T cells showed a significant defect in *IL-31* expression compared with wild-type CD4$^+$ T cells. In agreement with these findings, mice subjected to atopic conditions showed much higher levels of IL-31, which were closely correlated with a significant increase in the number of infiltrated NFAT1$^+$CD4$^+$ T cells into the AD ears. Amelioration of AD progression by cyclosporin A treatment was well correlated with downregulation of IL-31 expressions in CD4$^+$ T cells and total ear residual cells. In summary, our results suggest a functional cooperation between NFAT1 and JunB in mediating *IL-31* gene expression in CD4$^+$ T cells and indicate that interference with this interaction or their activity has the potential of reducing IL-31–mediated AD symptoms.** ***The Journal of Immunology*****, 2015, 194: 1963–1974.**

Interleukin-31 is produced by different immune cell types such as mast cells, eosinophils, epithelial cells, and by activated CD4$^+$ T cells and Th2 cells (1, 2). The IL-31 receptor is a heterodimeric receptor composed of IL-31RA and oncostatin M receptor-β (OSMR-β). Although IL-31 directly binds to IL-31RA, their binding affinity is significantly increased in the presence of OSMR-β. Binding of IL-31 to its receptor triggers JAK/STAT, MAPK, and PI3K/AKT pathways and activates STAT1, STAT3, and STAT5 transcription factors, which induce expression of diverse target genes (3–5) associated with various immune disorders. IL-31 regulates proliferation and survival of myeloid progenitor cells (6) and expression of proinflammatory cytokines and chemokines from nonimmune cells (7, 8). Increased expression of IL-31 correlates with pathogenesis of airway hypersensitivity by inducing the mediators such as vascular endothelial growth factor, epidermal growth factor, and CCL2 (8, 9). IL-31 also plays a pathogenic role in atopic dermatitis (AD) (10, 11), and its expression is closely correlated with the expression of IL-4 and IL-13 in AD patients (12–14). IL-31 transgenic mice spontaneously develop the symptoms of AD (2). Furthermore, enhanced levels of IL-31RA and OSMR-β are closely related with itching behavior in AD mice (15), and treatment with anti–IL-31 Ab inhibits the scratching behavior of the NC/Nga mouse (16).

The NFAT family consists of five members: NFAT1 (NFATc2), NFAT2 (NFATc1), NFAT3 (NFATc4), NFAT4 (NFATc3), and NFAT5 (TonEBP) (17). Activation of NFAT1 through NFAT4 is regulated by $Ca^{2+}$ signaling and NFAT1, NFAT2, and NFAT4 are expressed in immune cells. NFAT family members consist of NFAT homology region and REL homology region domains. The NFAT homology region domain contains calcineurin docking sites, nuclear localization sequence, and several inducible phosphorylation sites (18). The REL homology region serves as a DNA binding domain that contains Fos, Jun contact sites that allow the formation of NFAT, Fos/Jun, and a DNA quaternary complex. Increased $Ca^{2+}$ concentration by TCR engagement activates calmodulin and then sequentially activates the phosphatase calcineurin. Activated calcineurin dephosphorylates NFAT in the cytosol, which leads to nuclear translocation. NFAT positively regulates expression of various cytokines (19) by binding to the regulatory elements of its target gene loci through a formation of activation complexes with other transcription factors, including AP-1, CEBP, GATA3, T-bet, and IFN regulatory factor 4 (20, 21).

Although pathophysiological function of IL-31 in diverse immune disorders has been suggested, the molecular mechanisms responsible for *IL-31* gene expression in CD4$^+$ T cells and its relevance under AD remain elusive. In the present study, we identified the transcription start site, functional promoter region, and transcription

*Academy of Immunology and Microbiology, Institute for Basic Science, Pohang 790-784, Republic of Korea; †School of Life Sciences, Gwangju Institute of Science and Technology, Gwangju 500-712, Republic of Korea; ‡Division of Integrative Biosciences and Biotechnology, Pohang University of Science and Technology, Pohang 790-784, Republic of Korea; and §Department of Neurosurgery, Chosun University College of Medicine, Gwangju 501-717, Republic of Korea

Received for publication July 21, 2014. Accepted for publication December 14, 2014.

This work was supported by a research program of the Institute for Basic Science (Grant IBS-R005-G1-2014-a00) and by Agricultural Science and Technology Development Grant PJ907153, National Academy of Agricultural Science, Rural Development Administration, Republic of Korea.

Address correspondence and reprint requests to Dr. Sin-Hyeog Im, Academy of Immunology and Microbiology, Institute for Basic Science/Division of Integrative Biosciences and Biotechnology, Pohang University of Science and Technology, 77 Cheongam-Ro, Nam-Gu, Pohang 790-784, Republic of Korea. E-mail address: iimsh@postech.ac.kr

The online version of this article contains supplemental material.

Abbreviations used in this article: AD, atopic dermatitis; CA, constitutively active; ChIP, chromatin immunoprecipitation; CsA, cyclosporin A; DAPA, DNA affinity purification assay; DNCB, 2,4-dinitrochlorobenzene; HPRT, hypoxanthine phosphoribosyltransferase; KO, knockout; mt, mutated; NGS, normal goat serum; OSMR-β, oncostatin M receptor-β; PLA, proximity ligation assay; qRT-PCR, quantitative RT-PCR; siRNA, small interfering RNA; TSS, transcription start site; WT, wild-type.

factors responsible for *IL-31* gene expression in CD4$^+$ T cells. We showed that recruitment of NFAT1 and JunB proteins to the IL-31 promoter locus significantly enhanced IL-31 promoter activity. In experimental AD, infiltrated CD4$^+$ T cells that produce high levels of IL-31 expression also showed high NFAT1 levels. Additionally, oral administration of cyclosporin A (CsA) to AD mice significantly suppressed disease progression by decreasing IL-31 expression in CD4$^+$ T cells as well as total ear residual cells.

## Materials and Methods

### *Mice and cell lines*

Female BALB/c mice (6–8 wk of age) and C57BL/6 mice (6–8 wk of age) were purchased from Japan SLC (Hamamatsu, Japan). An NFAT1-deficient mouse line was provided by Dr. A. Rao (La Jolla Institute for Allergy and Immunology). All mice were maintained under specific pathogen-free conditions in the Animal Facility of the Gwangju Institute of Science and Technology. All experimental procedures were performed in accordance with National Institutes of Health's *Guidelines for the Care and Use of Laboratory Animals* and were approved by the Animal Care and Ethics Committees of the Gwangju Institute of Science and Technology (permit no. GIST-2011-3). Animals were maintained in accordance with the National Animal Welfare Law of Korea. The murine T cell lymphoma cell line EL4 was obtained from the Korea Cell Line Bank (Seoul National University, Seoul, Korea). Human embryonic kidney cell line HEK-293 was purchased from Invitrogen (Grand Island, NY).

### *Cell culture and stimulation*

Isolated primary cells were cultured in RPMI 1640 medium (Welgene, Daegu, Korea) supplemented with 10% FBS (HyClone Laboratories, Logan, UT), 3 mM L-glutamine (Sigma-Aldrich, St. Louis, MO), 100 U/ml penicillin (Sigma-Aldrich), 100 U/ml streptomycin (Sigma-Aldrich), nonessential amino acids (Welgene), sodium pyruvate (Welgene), HEPES (Welgene), and 0.05 mM 2-ME (Sigma-Aldrich). Ear total cells were cocultured with CD4$^+$ T cell–depleted splenocytes with house dust mite extracts (5 μg/ml) for 24 h. CD4$^+$ T cells were stimulated with PMA (50 ng/ml) and/or ionomycin (1 μM) for 2 h. CD4$^+$ T cells were also stimulated with 1 μg/ml plate-bound anti-CD3 (BD Biosciences, San Diego, CA), 1 μg/ml soluble anti-CD28 (BD Biosciences), or anti-CD3/anti-CD28 for 2 h. To check IL-31 mRNA expression kinetics, cells were stimulated with PMA/ionomycin or anti-CD3/anti-CD28 for the indicated time points. NFAT1-deficient CD4$^+$ T cells were stimulated with PMA/ionomycin for indicated time points to compare IL-31 expression with normal CD4$^+$ T cells. For the inhibitor experiments, CD4$^+$ T cells isolated from C57BL/6 mice or AD-induced mice were pretreated with 1 μM CsA (Calbiochem, Darmstadt, Germany), 5 μM tanshinone IIA (Santa Cruz Biotechnology, Santa Cruz, CA), CsA/tanshinone IIA, or actinomycin D (Sigma-Aldrich) for 30 min, then stimulated with PMA/ionomycin for an additional 2 h.

### *Isolation of CD4$^+$ T cells and total ear residual cells*

CD4$^+$ T cells from the lymph nodes and spleen of C57BL/6 mice were isolated with CD4$^+$ T cell isolation beads (Miltenyi Biotec, Bergish Gladbach, Germany) according to the manufacturer's protocol. Ears were removed from normal or AD groups, cut into three pieces, washed with RPMI 1640 medium (Welgene), and gently stirred in flasks containing 25 ml 1.0 mM EDTA in 5% FBS (HyClone Laboratories) for 20 min at room temperature. Then ear segments were minced, transferred into a 50-ml centrifuge tube containing 15 ml RPMI 1640 without serum, and vigorously shaken for 15 s three times. After that, tissues were transferred into T flasks containing 10 ml 0.5 mg/ml collagenase type V (Sigma-Aldrich) and incubated for 1 h at 37°C in a shaking incubator. Finally, the soup containing ear total cells was centrifuged and washed with ice-cold PBS and cultured in T cell media. Ear residual CD4$^+$ T cells were isolated with CD4$^+$ T cell isolation beads according to the manufacturer's protocol, and flow-through was used as non–CD4$^+$ T cells.

### *RACE*

5′-RACE was carried out by using the SMARTer RACE cDNA amplification kit (Clontech Laboratories, Mountain View, CA) according to the manufacturer's instructions. The primer sequences used are as follows: first PCR (5′-CCA CTT CCA GTC CCT ACA GGG TAG CAG AAC AAG ATT TCA-3′), nested PCR (5′-TAA CAT GAC TAG TAA TGA CCG CAC AGT-3′). The resulting RACE PCR products were isolated from agarose gel by using the NucleoTrap gel extraction (Clontech), cloned into pGEM-T Easy vector (Promega, Madison, WI), and confirmed by sequencing.

### *RNA isolation, cDNA synthesis, and quantitative real-time PCR*

Total RNA was extracted from cells with TRIzol reagent (Molecular Research Center, Cincinnati, OH) according to the manufacturer's protocol. For reverse transcription, 1 μg total RNA was used and cDNA was generated using an oligo(dT) primer (Promega) and ImProm-II reverse transcriptase (Promega) in a total volume of 20 μl. The mRNA level was determined using 1 μl cDNA by real time PCR with SYBR Green using a protocol provided by the manufacturer (Chromo4; MJ Research). Mouse hypoxanthine phosphoribosyltransferase (HPRT) primer was used for quantitative RT-PCR (qRT-PCR) to normalize the amount of cDNA used for each condition. The primer sequences used are as follows: HPRT (forward, 5′-TTA TGG ACA GGA CTG AAA GAC-3′; reverse, 5′-GCT TTA ATG TAA TCC AGC AGG T-3′), IL-31 (forward, 5′-ACA ACT ATA GCA TAA AGC AGG C-3′; reverse, 5′-GAT TCA TCA GTA TTT CCA GGC A-3′), NFAT1 (forward, 5′-GAG AAG ACT ACA GAT GGG CAG-3′; reverse, 5′-ACT GGG TGG TAG GTA AAG TG-3′), and JunB (forward, 5′-AGG TGA AGA CAC TCA AGG CTG AGA A-3′; reverse, 5′-TGA CAT GGG TCA TGA CCT TCT GCT T-3′).

### *Plasmid construction, site-directed mutagenesis, and luciferase reporter assays*

The deletion constructs were generated by cloning the genomic sequences upstream of the first coding exon of the *IL-31* gene into the pXPG reporter vector digested by appropriate restriction enzymes. Different combinations of forward primers and same reverse primer in the 5′ region of the transcription start site of the mouse IL-31 were used to obtain the deletion constructs and primer sequences as follows: forward, 2276 bp, 5′-CGC GGA TCC GCC TGA AAG ATG CTA TGT AAT CC-3′; 1461 bp, 5′-CGC GGA TCC ATT AAG TAC TGA AGT AGG GCT-3′; 767 bp, 5′-GGA AGA TCT TCC CAT AAT TAA CTG ATC CAC C-3′; 498 bp, 5′-GGA AGA TCT CCC TCT AAG TCA CTT CTT CC-3′; 381 bp, 5′-GGA AGA TCT GTG GTA TGT GTA TGC GTT TGT G-3′; 257 bp, 5′-GGA AGA TCT CTG GCA ACC TTT TGA AAA TG-3′; 194 bp, 5′-GGA AGA TCT CTT TGA TCT GCT TCC TCA TGA C-3′; reverse, 5′-CCC AAG CTT CCC TAA CAT GAT AAG AGC CA-3′. The sequences of all the PCR-derived constructs were confirmed by DNA sequencing. The binding sites for NFAT1 or AP-1 (JunB) in the IL-31 promoter locus were subjected to site-directed mutagenesis. Primers used for the generation of mutant constructs are as follows (mutated regions are underlined): mutated (mt) NFAT-a, forward, 5′-GCA ACC TTT TGA AAA TGT GGG CTG GAG AAA AGC TGA GC-3′, reverse, 5′-GCT CAG CTT TTC TCC AGC CCA CAT TTT CAA AAG GTT GC-3′; mtNFAT-b, forward, 5′-GAA AAT GTT TTC GTT AGA AAA GCT GAG C-3′, reverse, 5′-GCT CAG CTT TTC TAA CGA AAA CAT TTT C-3′; mtNFAT-c, forward, 5′-GAG AAA AGC TGA GCA ATG GTG GGG CCA TGG GCG GGC CTT TGA TC-3′, reverse, 5′-GAT CAA AGG CCC GCC CAT GGC CCC ACC ATT GCT CAG CTT TTC TC-3′; mtAP-1–a, forward, 5′-CTT TCC TCT CAT TAA AGA CGC AAG CAC TTT CCA AG-3′, reverse, 5′-CTT GGA AAG TGC TTG CGT CTT TAA TGA GAG GAA AG-3′; mtAP-1–b, forward, 5′-GTT TTC TGG AGA AAA GCG TCT CAA TGG TTT TGC CAT GGG-3′, reverse, 5′-CCC ATG GCA AAA CCA TTG AGA CGC TTT TCT CCA GAA AAC-3′. Plasmid DNAs were prepared by Gene All Exprep Plasmid SV kit (GeneAll Biotechnology, Seoul, Korea) and EL4 T cells were transiently transfected by GeneExpresso (Excellgen, Rockville, MD) according to the manufacturers' protocols. The total amount of transfected DNA for each sample was normalized by adding the control vector, pcDNA. After 18 h, cells were stimulated with PMA/ionomycin for 6 h and then luciferase activity was accessed by the Dual-Luciferase assay system (Promega, Madison, WI). Cotransfection of the HRE-luciferase vector as an internal control allowed normalization of transfection by *Renilla* luciferase activity. Constitutively active (CA)-NFAT1– and mtCA-NFAT1–expressing vectors were given to us by Dr. A. Rao (La Jolla Institute for Allergy and Immunology). CA-NFAT1 or mtCA-NFAT1 construct was transfected with the IL-31 promoter containing reporter plasmid to EL4 T cells in the presence or absence of JunB expression vector, and following steps are same as previously described.

### *Proximity ligation assay*

The in situ PLA proximity ligation assay (PLA; Duolink in situ fluorescence kit, Olink Bioscience, Uppsala, Sweden) was used to detect the interaction between NFAT1 and JunB in CD4$^+$ T cells. Wild-type (WT) CD4$^+$ T cells or NFAT1 knockout (KO) CD4$^+$ T cells were stimulated with or without PMA/ionomycin, followed by fixation with PFA, permeabilized, and incubated with the indicated primary Abs and the PLA probes (anti-murine and anti-rabbit IgG Abs conjugated with oligonucleotides). Ligation and

amplification were performed according to the manufacturer's instructions. Imaging was performed on fixed samples with a confocal laser scanning microscope Zeiss LSM 700 (×63 oil immersion objective).

### *Chromatin immunoprecipitation assay*

Chromatin immunoprecipitation (ChIP) analysis was carried out essentially as described (22) with minor modifications. $CD4^+$ T cells isolated from WT and NFAT1-deficient mice were harvested and fixed with formaldehyde after treating with or without PMA/ionomycin for 2 h prior to harvest. Chromatin was immunoprecipitated using anti-NFAT1 Ab (Santa Cruz Biotechnology), anti-JunB Ab (Santa Cruz Biotechnology), or rabbit IgG Ab (Sigma-Aldrich). Following reversal of crosslinks, presence of the selected DNA sequence was assessed by real-time PCR using SYBR Freen PCR mix. The primer sequences used in ChIP are as follows: −359/−242 region, forward, 5′-CCC TCT AAG TCA CTT CTT CC-3′, reverse, 5′-CAA GGC AGA AGA TTG AGT CAC-3′; −116/−53 region, forward, 5′-ATC TTC TGC CTT GCC TTG AG -3′, reverse, 5′-ATG AGG AAG CAG ATC AAA GG-3′; −1374/−1179 region, forward, 5′-AAA TAA AGA GTC GTT CAG CCA GG-3′, reverse, 5′-AGT GAT CAA TTA GCC CAG CCT-3′. As a loading control, the PCR was done directly on input DNA purified from chromatin before immunoprecipitation. Data are presented as the amount of DNA recovered relative to the input control.

### *DNA affinity purification assay*

A DNA affinity purification assay (DAPA) was performed following protocols described previously with minor modifications (21). Briefly, biotinylated complementary oligonucleotides were annealed in TEN (10 mM Tris/HCl [pH 8.0], 1 mM EDTA, 100 mM NaCl) buffer. HEK-293 cells overexpressing NFAT1 or JunB were lysed by sonication in 200 μl HKMG (10 mM HEPES [pH 7.9], 100 mM KCl, 5 mM $MgCl_2$, 10% glycerol, 0.1% Nonidet P-40, and 1 mM DTT) buffer containing protease and phosphatase inhibitors (Roche Applied Science). The cellular debris was removed by centrifugation. After that 30 μg total cell lysate was incubated with anti-NFAT1, anti-JunB, and anti–β-actin (Abcam, Cambridge, MA) Abs to check the expression level of NFAT1 and JunB along with that of actin (control) by immunoblotting. The cell extracts (500 μg) were precleared with 10 μl M-280 streptavidin beads (Invitrogen) for 1 h at 4˚C with gentle agitation. The cleared nuclear extracts were then incubated with 1 μg biotinylated double-stranded probes and 10 μg poly(dI-dC) overnight. Ten microliters M-280 streptavidin beads was used to pull down bound proteins for 1 h at 4˚C with gentle agitation. The beads were washed four times with cold HKMG buffer. SDS sample buffer was then added to the beads. The samples were boiled for 5 min and subjected to SDS-PAGE and Western blotting with anti-NFAT1 and anti-JunB (Santa Cruz Biotechnology) Abs. Blots were developed using HRP-conjugated secondary Ab (Sigma-Aldrich) and the an ECL Western blot detection kit (Amersham Pharmacia Biotech, Arlington Heights, IL). The probe sequences used for DAPA are as follows: NFAT-a, forward, 5′-CAA GCA CTT TCC AAG AAA AGA GAG ATG C-3′, reverse, 5′-GCA TCT CTC TTT TCT TGG AAA GTG CTT G-3′; NFAT-b, forward, 5′-CAA CCT TTT GAA AAT GTT TTC TGG AGA AAA-3′, reverse, 5′-TTT TCT CCA GAA AAC ATT TTC AAA AGG TTG-3′; NFAT-c, forward, 5′-AAG CTG AGC AAT GGT TTT GCC ATG GGC GGG-3′, reverse, 5′-CCC GCC CAT GGC AAA ACC ATT GCT CAG CTT-3′; NFAT consensus, forward, 5′-CCC AAA GAG GAA AAT TTG TTT CAT-3′, reverse, 5′-ATG AAA CAA ATT TTC CTC TTT GGG-3′; AP-1–a, forward, 5′-TCC TCT CAT TAA ATC AGC AAG CAC TTT CCA-3′, reverse, 5′-TGG AAA GTG CTT GCT GAT TTA ATG AGA GGA-3′; AP-1–b, forward, 5′-TCT GGA GAA AAG CTG AGC AAT GGT TTT G-3′, reverse, 5′-CAA AAC CAT TGC TCA GCT TTT CTC CAG A-3′; mtNFAT-a, forward, 5′-CAA GCA CGG GCC AAG AAA AGA GAG ATG C-3′, reverse, 5′-GCA TCT CTC TTT TCT TGG CCC GTG CTT G-3′; mtNFAT-b, forward, 5′-CAA CCT TTT GAA AAT GTT TTC GTT AGA AAA-3′, reverse, 5′-TTT TCT AAC GAA AAC ATT TTC AAA AGG TTG-3′; mtNFAT-c, forward, 5′-AAG CTG AGC AAT GGT GGG GCC ATG GGC GGG-3′, reverse, 5′-CCC GCC CAT GGC CCC ACC ATT GCT CAG CTT-3′; mtAP-1–a, forward, 5′-TCC TCT CAT TAA AGA CGC AAG CAC TTT CCA-3′, reverse, 5′-TGG AAA GTG CTT GCG TCT TTA ATG AGA GGA-3′; mtAP-1–b, forward, 5′-TCT GGA GAA AAG CGT CTC AAT GGT TTT G-3′, reverse, 5′-CAA AAC CAT TGA GAC GCT TTT CTC CAG A-3′.

### *Small interfering RNA transfection assay*

The predesigned small interfering RNAs (siRNAs) for NFAT1 (sc-36056), JunB (sc-35727), and control siRNA (sc-37007) were purchased from Santa Cruz Biotechnology. For siRNA transfection, effector T cells were subjected to nucleofection (Amaxa Nucleofector; Lonza, Walkersville, MD) according to the manufacturer's protocol. Briefly, effector T cells were resuspended in mouse T cell nucleofection solution at a density of $2 \times 10^6$ per 100 μl. In each transfection, 100 μl cell suspension was mixed with 1 μM siRNA, transferred into a cuvette, and pulsed in a Nucleofector device using program X-001. The cells were then transferred into a 12-well plate and plated in 1 ml prewarmed medium. Forty-six hours after transfection, the cells were treated with PMA/ionomycin for 2 h and harvested. mRNA isolation and cDNA synthesis was performed following the protocol described before, and knockdown efficiency was determined by qRT-PCR and Western blot. Relative band intensity (intensity of NFAT1 or JunB/intensity of β-actin) of each sample was analyzed by ImageJ software. For ChIP analysis, effector T cells were transfected with control siRNA or JunB siRNA. Forty-six hours after transfection, the cells were stimulated with PMA/ionomycin for 2 h and harvested to perform an NFAT1 ChIP assay.

### *NFAT1 overexpression and reconstitution*

Isolated $CD4^+$ T cells from WT C57BL/6 or NFAT1-deficient mice were stimulated with anti-CD3/anti-CD28 in the presence of rIL-2 (100 U/ml) for 3 d, then cultured in only IL-2–containing complete T cell media. NFAT1, JunB, or NFAT1 and JunB were transfected into effector T cells by an Amaxa Nucleofector (Lonza) according to the manufacturer's protocol. After 22 h of transfection, cells were stimulated with PMA/ionomycin for 2 h and IL-31 mRNA level was measured by real-time PCR. In this experiment, GFP-expressing vector was used as a control. Protein expression levels of NFAT1 in WT $CD4^+$ T cells, NFAT1-deficient $CD4^+$ T cells, and NFAT1-reconstituted NFAT1-deficient $CD4^+$ T cells were measured by Western blot, and β-actin was used as a loading control. Relative band intensity (intensity of NFAT1/intensity of β-actin) of each sample was analyzed by ImageJ software.

### *Preparation of total cell lysate and nuclear extract*

Cells were washed with ice-cold PBS and resuspended in RIPA buffer (50 mM Tris-HCl [pH 8.0], 150 mM NaCl, 0.1% SDS, 0.5% sodium deoxycholate) containing protease inhibitors and 1% Nonidet P-40. Cells were allowed to swell by incubation on ice for 20 min, and then the homogenate was centrifuged for 5 min. The supernatant containing total cell lysate was transferred to new tubes and used for immunoblotting. Nuclear extract was prepared with NE-PER nuclear and cytoplasmic extraction reagents (Thermo scientific, Waltham, MA) according the to manufacturer's protocol. The supernatant containing nuclear extract was used for immunoblotting.

### *Induction of AD and treatment of CsA*

Induction of experimental AD was performed by following a protocol described previously (23). Briefly, surfaces of both ear lobes of female BALB/c mice (6–8 wk of age) were stripped five times with surgical tape (Nichiban, Tokyo, Japan). After stripping, 20 μl 2% 2,4-dinitrochlorobenzene (DNCB) (Sigma-Aldrich) dissolved in acetone/olive oil (1:3) solution was painted on each ear. After 3 d, 20 μl 10 mg/ml mite extract (*Dermatophagoides farinae*; GREER, Lenoir, NC) dissolving in PBS containing 0.5% Tween 20 was repainted. Challenge of DNCB and mite extract was repeated once a week alternatively until 5 wk. Only tape stripping and PBS painting were performed in the normal group. To examine the effect of CsA, the microemulsion form of CsA (5 mg/kg/d; Novartis, New York, NY) was orally administrated to BALB/c mice 5 d/wk for 4 wk during the period of AD induction. The same volume of DMSO was treated as a control.

### *Immunohistochemistry*

Ears from AD-induced mice, normal mice, control AD–induced mice, and CsA-treated AD-induced mice were fixed with 4% paraformaldehyde in PBS (pH 7.4). Fixed tissues were washed in sucrose solution with several changes (10% sucrose in PBS for 4 h, 15% sucrose in PBS for 4 h, and 20% sucrose in PBS overnight) and were frozen in OCT compound (Sakura Finetek, Leiden, The Netherlands). Cryostat sections (10 μm) were mounted on Superfrost Plus slides and dried overnight at room temperature. Slides were permeabilized with 0.1% Triton X-100 in 1% normal goat serum (NGS) for 15 min and then blocked with 5% NGS for 1 h at room temperature. After washing with TBS, sections were incubated overnight at 4˚C with the following primary Abs: mouse anti-NFAT1 mAb (1:50 in 1% NGS; Santa Cruz Biotechnology), rabbit anti–IL-31 mAb (1:50 in 1% NGS; Abcam, Cambridge, U.K.), and rat anti-CD4 mAb (1:100 in 1% NGS; Santa Cruz Biotechnology). They were then washed with TBS and the sections were incubated for 1 h at room temperature with the following corresponding secondary Abs: Alexa Fluor 405 goat anti-mouse IgG (1:1000; Invitrogen), Alexa Fluor 488 donkey anti-rabbit IgG (1:1000; Invitrogen), and Alexa Fluor 594 goat anti-rat IgG (1:1000; Invitrogen). Nucleus was counterstained with DAPI (1:3000; Invitrogen) for 5 min at room temperature. Sections were washed and then mounted with fluorescence mounting medium (Dako, Seoul, Korea).

*Computational analysis of the conserved nucleotide sequence locus*

To identify a potential regulatory locus, comparative genomic analysis was performed. Genomic sequences spanning the *IL-31* gene were analyzed using the Web-based alignment software VISTA browser 2.0 (23). Transcription factor binding sites were identified using the rVISTA 2.0 software (24), which uses matrices of the TRANSFAC database (25). Putative recognition sites for regulatory factors were also identified by searching the JASPAR database (26) and verified from previously reported literature.

*Statistical analysis*

A two-tailed Student *t* test was used. A $p$ value $<0.05$ was considered statistically significant.

## Results

*TCR stimulation–dependent* IL-31 *gene expression*

To investigate the underlying mechanism of *IL-31* gene expression in CD4$^+$ T cells, we analyzed the IL-31 mRNA expression profile. CD4$^+$ T cells isolated from spleen and lymph nodes of C57BL/6 mice were either unstimulated or stimulated with TCR signaling (anti-CD3/anti-CD28) or PMA/ionomycin, along with related controls. Relative levels of IL-31 mRNA expression were analyzed by qRT-PCR. IL-31 expression was significantly increased upon anti-CD3/anti-CD28 or PMA/ionomycin stimulation (Fig. 1A). To test whether IL-31 expression is regulated at the transcriptional level, we tested the effect of actinomycin D, an inhibitor of mRNA synthesis. Indeed, pretreatment with actinomycin D significantly decreased IL-31 mRNA expression upon PMA/ionomycin stimulation (Fig. 1B). Next, we determined the expression kinetics of IL-31 mRNA expression. CD4$^+$ T cells were stimulated with anti-CD3/anti-CD28 or PMA/ionomycin for the indicated time points. Stimulation with PMA/ionomycin or anti-CD3/anti-CD28 for 2 h significantly increased IL-31 expression (PMA/ionomycin, 290-fold; anti-CD3/anti-CD28, 105-fold) (Fig. 1C) measured by qRT-PCR, and relative expression level was visualized as the agarose gel image (Fig. 1D). These results suggest that IL-31 expression is regulated through TCR signaling at the transcription level.

*Identification of the transcription start site and promoter region*

To identify the transcription start site (TSS) at the mouse *IL-31* gene locus, we employed the SMART 5′-RACE technique. mRNA isolated from CD4$^+$ T cells was amplified with the gene-specific primer (corresponds to the exon 3 region of the *IL-31* gene) and the universal primer mix (Fig. 2A). RACE PCR produced one major IL-31 transcript in CD4$^+$ T cells (Fig. 2B). To determine the location of the TSS, RACE transcript was isolated, sequenced, and alignment of the sequenced RACE products to the mouse genome was performed along with GenBank (GenBank accession no. NM029594; http://www.ncbi.nlm.nih.gov/nuccore/NM_029594.1). TSS was aligned with 60 bp upstream of translation start site, ATG (Fig. 2C). Next, to identify the potential regulatory elements in the 5′ region of the *IL-31* gene, we performed a comparative genomic sequence analysis. rVISTA 2.0 and TRANSFAC database analysis revealed several potential regulatory elements that have highly conserved noncoding sequences between humans and mice (Fig. 3A). These include TSS, TATA box, and predicted transcription factor binding sites (Fig. 3B). To identify the core *cis*-regulatory elements we generated a series of deletion constructs as depicted in Fig. 3C. DNA fragments encompassing various 5′ upstream regions of the *IL-31* gene were cloned into the luciferase reporter vector (Fig. 3C). These constructs were transiently transfected into EL4 T cells, and their relative reporter activities were compared. The functional promoter region was mapped in the −359/+141 region (498-bp construct) that showed maximal promoter activity upon PMA/ionomycin stimulation (Fig. 3C). Interestingly, further deletion of the functional promoter region significantly decreased its promoter activity as shown in the −242/+141 region (381-bp construct) and the −53/+141 region (194-bp construct), suggesting that the −359/+141 region may serve as a core *IL-31* promoter in CD4$^+$ T cells.

*Functional cooperation between NFAT1 and JunB to activate IL-31 expression*

To identify the key transcription factors responsible for TCR stimulation–dependent *IL-31* promoter activity, we performed sequence analysis of the identified −359/+141 functional promoter region of the *IL-31* gene. Indeed, we could identify highly conserved binding sites for AP-1, NFAT, and NF-κB (Fig. 3B). To delineate which transcription factors play a major role in activation of *IL-31* promoter, a luciferase reporter assay was performed in the presence of different combinations of transcription factors.

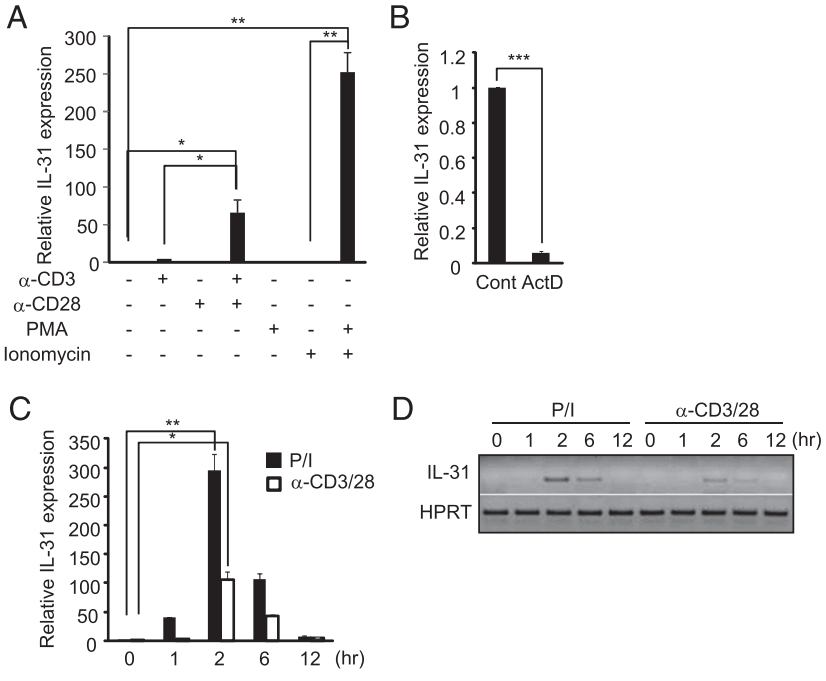


**FIGURE 1.** TCR stimulation induces IL-31 expression in CD4$^+$ T cells. (**A**) CD4$^+$ T cells were stimulated under indicated conditions and relative IL-31 expression level was measured by qRT-PCR analysis. (**B**) CD4$^+$ T cells pretreated with actinomycin D (ActD) for 30 min were stimulated with PMA/ionomycin for 2 h, and relative IL-31 expression level was measured by RT-PCR. (**C**) CD4$^+$ T cells were stimulated with anti-CD3/anti-CD28 or PMA/ionomycin (P/I) for indicated time points and then subjected to qRT-PCR analysis. Mouse HPRT was used as an internal control, and relative IL-31 level compared with control sample is presented in (A) through (C). (**D**) IL-31 and HPRT mRNA expressions were analyzed by qRT-PCR upon stimulation and were visualized in agarose gel. Error bars indicate SD. Data are representative of three independent experiments. *$p < 0.05$, **$p < 0.005$, ***$p < 0.001$.

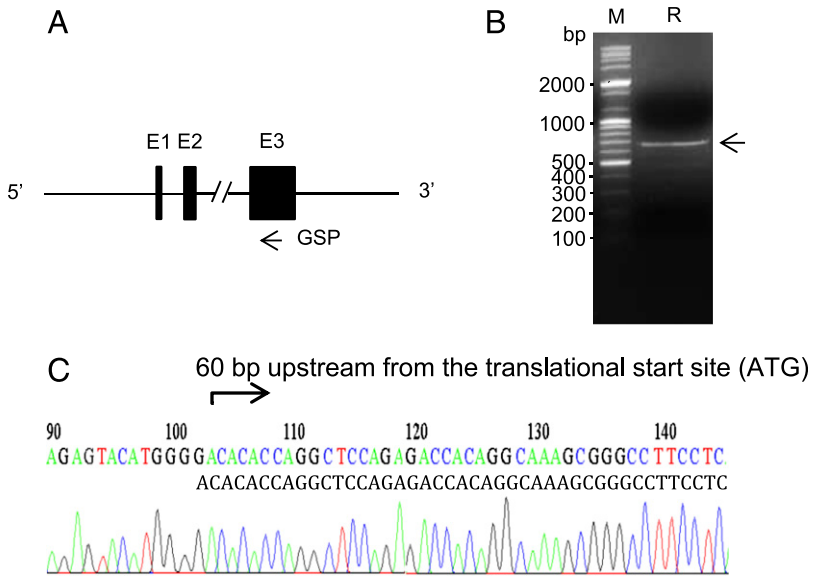


**FIGURE 2.** Determination of the transcription start site of the *IL-31* gene locus. (**A**) Schematic diagram of RACE analysis. The positions of exons (E) in *IL-31* genomic locus are shown. The gene specific primer (GSP, arrow) used in 5′-RACE is located in exon 3 (E3). (**B**) After performing 5′-RACE, the PCR product was analyzed and its size was determined by arose gel electrophoresis (black arrow). (**C**) The 5′-RACE product was cloned into the pGEM-T vector and sequenced. Analyzing the DNA sequence (GenBank accession no. NM029594) revealed a major TSS assigned to the G nucleotide 60 bp upstream of the translation start site (ATG). Data are representative of three independent experiments. M, marker; R, RACE product.

EL4 T cells were transiently transfected with an IL-31 promoter–driven luciferase construct along with empty vector, vectors encoding members of the AP-1 family (JunB, c-Jun, and c-Fos), or NFAT family (NFAT1, NFAT2, and NFAT4). Among them, NFAT1 overexpression significantly enhanced IL-31 promoter activity (Fig. 4A) in a dose-dependent manner (Fig. 4B). However, other factors such as NFAT2, NFAT4, JunB, c-Jun, and c-Fos failed to activate the IL-31 promoter (Fig. 4A). Because NFAT protein functions with other interacting partners to regulate its target gene expression (27), we tested whether NFAT1 could further enhance its IL-31 transcriptional activity through a coordinate interaction with AP-1 protein that has a binding site near the NFAT binding site at the IL-31 promoter (Fig. 3B). An IL-31 promoter–driven luciferase construct was transfected with NFAT1 alone or in combination with each family of AP-1 proteins, and transactivity was measured by a luciferase assay. Cotransfection of NFAT1 and JunB synergistically increased promoter activity compared with the activity of single transfection (Fig. 4C). Even though c-Jun and c-Fos also showed

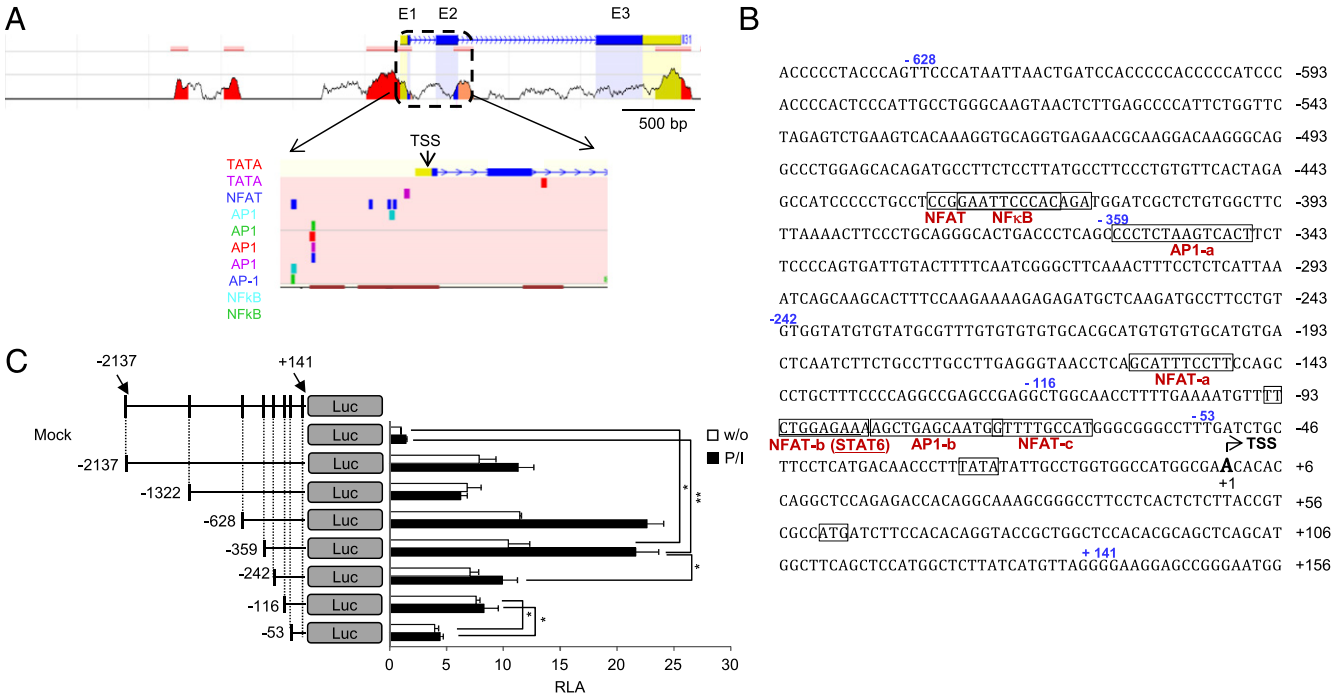


**FIGURE 3.** Identification of the functional promoter region of the *IL-31* gene. (**A**) ECR browser analysis of the mouse and human *IL-31* loci is shown. The mouse genomic sequence is used as the base sequence on the *x*-axis. Schematic representation of the genomic positions of exons (E) and putative binding sites of transcription factors and TATA box in the 5′-end region of the *IL-31* gene are shown. (**B**) 5′-End genomic sequence of mouse *IL-31* gene locus with TSS indicated in bold type and black arrow and designated as +1. Locations of the deletion constructs are indicated in blue. TATA box (TATA), translation start site (ATG), and putative binding sites for transcription factors (AP-1, NFAT, and NF-κB) are indicated and boxed. STAT6 binding site in the human IL-31 promoter is underlined in red. (**C**) EL4 T cells were transfected with the control mock vector or indicated deletion constructs. Cells were unstimulated or stimulated with PMA/ionomycin for 6 h and then relative luciferase activity (RLA) was expressed as fold difference relative to the unstimulated mock sample. The genomic location and size of each deletion construct are specified. Error bars indicate SD. Data are representative of three independent experiments. $^{*}p < 0.05$, $^{**}p < 0.005$.

a synergistic effect with NFAT1 in IL-31 promoter activity, JunB showed a more significant effect compared with other AP-1 proteins. Therefore, we decided to focus on the synergistic effect between NFAT1 and JunB for IL-31 gene expression. We also tested whether STAT6 could activate the mouse IL-31 promoter because STAT6 was reported as a key transcription factor for enhancing the human IL-31 promoter activity (24). Unlike in the human IL-31 promoter, NFAT2 and STAT6 failed to activate the mouse IL-31 promoter, and NFAT1 alone sufficiently activated the mouse IL-31 promoter in a STAT6-independent manner (Supplemental Fig. 1B). Overexpression of constitutively active form of NFAT1 (25) enhanced IL-31 promoter activity and cotransfection of CA-NFAT1 and JunB further enhanced IL-31 promoter activity. However, cotransfection of mtCA-NFAT1 (25), a mutant CA-NF1 that has a mutation in the AP-1 binding sites, with JunB failed to exert a functional synergism (Fig. 4D). Deletion of NFAT and AP-1 binding sites in the functional promoter (−359/−116 region) significantly reduced its promoter activity as observed in the −116/+141 region (257-bp construct) reporter vector (Fig. 4E). To further confirm the importance of NFAT and AP-1 transcription factors on IL-31 promoter activity, NFAT or AP-1 (JunB) binding sites were mutated in the functional promoter (−359/+141 region) individually or in combination as shown in Fig. 4F. Promoter activity was significantly decreased when a mutation was introduced in the NFAT binding site located in the −359/−116 region and −116/+141 region. In the case of AP-1 (JunB), single mutation of each AP-1 binding site decreased the promoter activity. Interestingly, IL-31 promoter activity was significantly reduced when all of the NFAT and AP-1 binding sites were mutated (Fig. 4F). These results suggest that although NFAT1 plays a major role in activation of IL-31 promoter, AP-1 (JunB) provided an additive effect on TCR-induced IL-31 promoter activity.

### *Physical binding of NFAT1 and JunB to the IL-31 promoter locus*

To test whether the functional synergism between NFAT1 and JunB results from protein–protein interaction between them, we performed a PLA in CD4$^+$ T cells. Under unstimulated condition, a PLA signal was detected only in the cytoplasmic region, and more distinct signals were observed in the nucleus upon PMA/ionomycin stimulation (Fig. 5A). In contrast, there was no detectable PLA signal when WT CD4$^+$ T cells were incubated with only NFAT1 Ab (Fig. 5B) or NFAT1 KO CD4$^+$ T cells that were incubated with both NFAT1 and JunB Abs (Fig. 5C). These results suggest that NFAT1

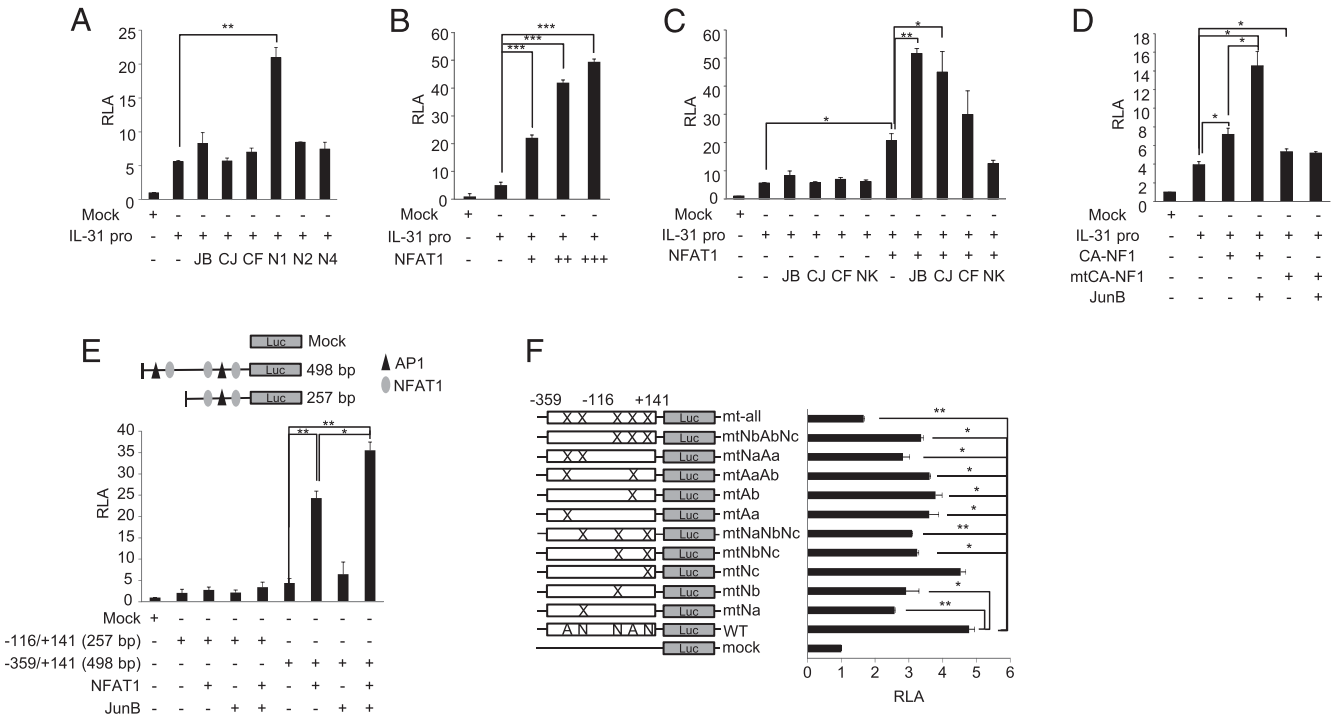


**FIGURE 4.** NFAT1 and JunB cooperatively transactivate the IL-31 promoter. (**A**–**C**) EL4 cells were transfected with control vector (mock) or luciferase reporter constructs driven by the IL-31 promoter (−359/+141 region, 498-bp construct) along with expression plasmids encoding NFATs (NFAT1 [N1], NFAT2 [N2], and NFAT4 [N4]), AP-1 (JunB [JB], c-Jun [CJ], and c-Fos [CF]), and NF-κB (p65) (NK) or their combinations as indicated. Cells were stimulated with PMA/ionomycin for 6 h and harvested for luciferase assay. (**B**) The NFAT1 dose-dependent effect was analyzed (300 [+], 600 [++], and 900 [+++] ng). Cells were stimulated with PMA/ionomycin for 6 h and harvested for the luciferase assay. (**D**) EL4 cells were transfected with luciferase reporter construct driven by the IL-31 promoter along with expression plasmids encoding CA-NFAT1 (CA-NF1) or mtCA-NFAT1 (mtCA-NF1, which has mutations in AP-1 binding site) in the presence or absence of JunB-expressing plasmid, as indicated. Cells were stimulated with PMA/ionomycin for 6 h and harvested for the luciferase assay. Relative luciferase activity (RLA) of each sample to control sample (mock) is presented. (**E**) The 257-bp construct (−116/+141 region) or 498-bp construct (−359/+141 region) was transfected to EL4 cells along with the indicated expression plasmids, stimulated with PMA/ionomycin, and then the relative luciferase assay was measured. The binding sites for AP-1 (filled triangle) or NFAT (gray-filled circle) are shown. (**F**) Various combinations of mutations were introduced into the IL-31 promoter reporter construct as indicated; X, mutated site in NFAT1 (N) or JunB (A) binding sites in Fig. 3*B*: mtNa, mtNb, mtNc, mtNbNc, and mtNaNbNc indicate mutations in the NFAT binding sites alone or in combination in NFAT-a, NFAT-b, and NFAT-c, respectively; mtAa, mtAb, and mtAaAb indicate mutations in the AP-1 binding sites alone or in combination in AP-1–a and AP-1–b, respectively; mtNaAa indicates mutations in NFAT-a and AP-1–a; mtNbAbNc indicates mutations in NFAT1-b, AP-1–b and NFAT-c; mt-all indicates mutations in all of the AP-1 and NFAT1 binding sites. Each mutant construct was transfected in EL4 cells, stimulated with PMA/ionomycin for 6 h, and then the RLA was measured. RLA activity was expressed as a fold difference relative to the control sample (mock). Error bars indicate SD. Data are representative of three independent experiments. *$p < 0.05$, **$p < 0.005$, ***$p < 0.001$.

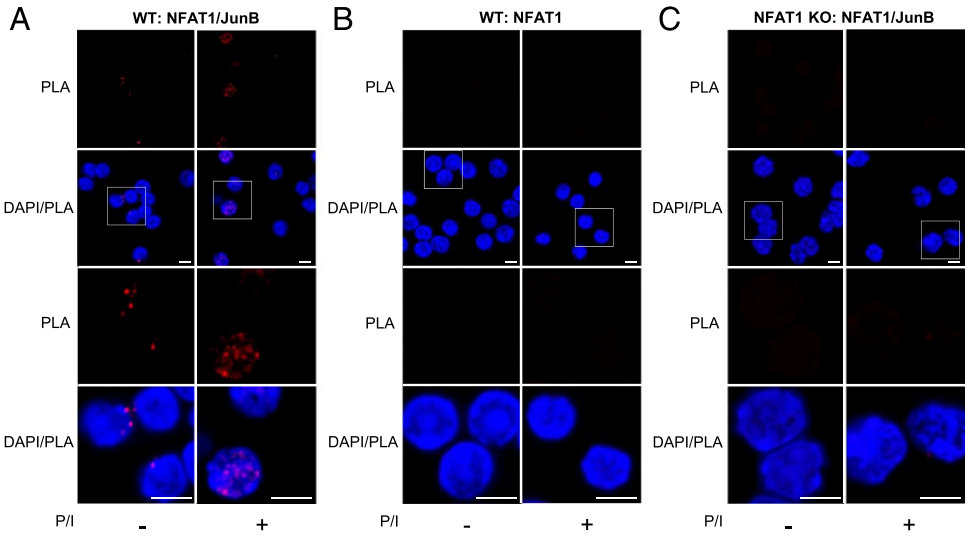


**FIGURE 5.** Physical interaction between NFAT1 and JunB in primary CD4$^+$ T cells. (**A**) NFAT1/JunB association was visualized in WT CD4$^+$ T cells with an in situ proximity ligation assay as described in *Materials and Methods*. CD4$^+$ T cells were stimulated with (+) or without (−) PMA/ionomycin (P/I) for 2 h, after which they were subjected to PLA. Red staining indicates an NFAT1/JunB interaction, and DAPI was used to visualize the nuclei (blue). (**B**) WT CD4$^+$ T cells were treated as described in (A) without anti-JunB Ab. (**C**) NFAT1 KO CD4$^+$ T cells were used and all of the procedures were same as is (A). The *top panels* are overviews at lower magnification, whereas in the *lower panels* images are shown at a higher magnification of the white square in the *upper panels*. Images are representative of three independent experiments. Scale bars, 5 μm.

and JunB interact in primary CD4$^+$ T cells. Following this, to detect a physical binding of NFAT1 to the predicted NFAT binding sites on the IL-31 promoter, we performed ChIP experiments using Abs for NFAT1 and JunB. In vivo binding of NFAT1 (Fig. 6A) and JunB (Fig. 6B) to the −359/−116 and −116/−53 region was confirmed in CD4$^+$ T cells, and their binding to the loci was further enhanced

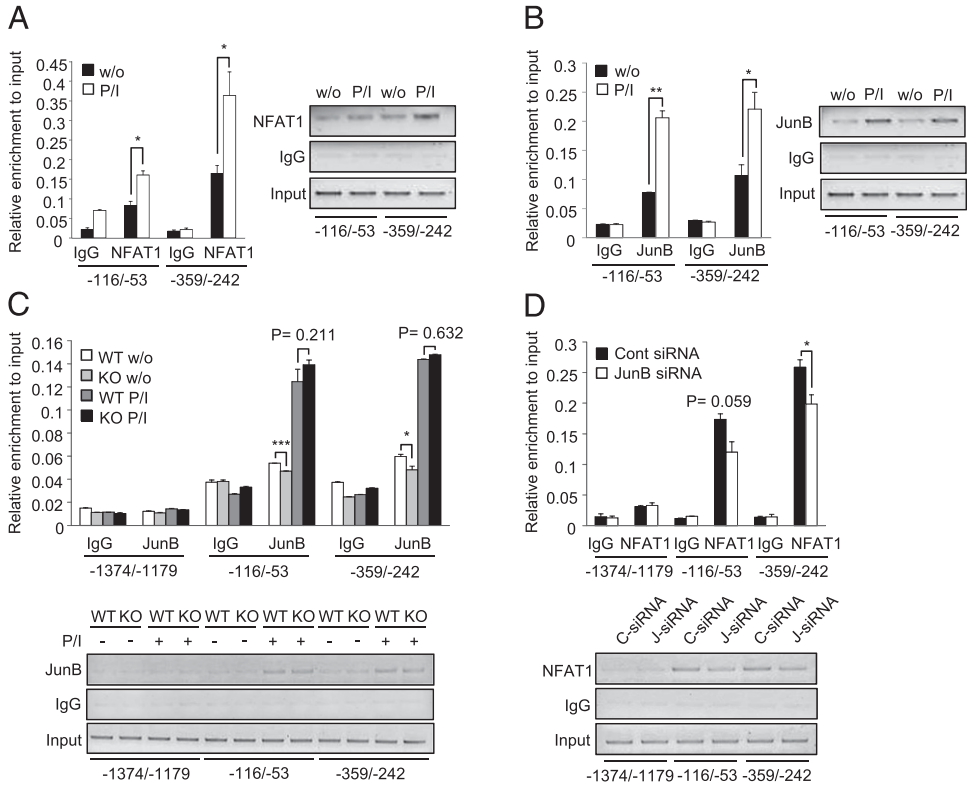


**FIGURE 6.** In vivo binding of NFAT1 and JunB to the *IL-31* promoter locus. (**A** and **B**) ChIP assay was performed with unstimulated (w/o) or PMA/ionomycin-stimulated (P/I) CD4$^+$ T cells using control IgG, anti-NFAT1 Ab (A) or anti-JunB Ab (B). (**C**) ChIP assay was performed with unstimulated (w/o) or PMA/ionomycin-stimulated (P/I) CD4$^+$ T cells isolated from WT or NFAT1 KO mice using control IgG or anti-JunB Ab. (**D**) Activated T cells were transfected with control or JunB siRNA. After 46 h of transfection, cells were stimulated with PMA/ionomycin for 2 h and harvested to analyze NFAT1 binding. The amounts of precipitated DNA were measured by qRT-PCR with primers specific for the indicated NFAT/JunB binding regions (−116/−54, −359/−242) in the IL-31 promoter locus (A–D) and negative control locus (−1374/−1179) (C and D). Relative enrichment of the IL-31 promoter in the precipitated samples compared with total chromatin (input) is shown. Negative images of ethidium bromide–stained gels are also shown in the *right panel*. C-siRNA, control siRNA; J-siRNA, JunB siRNA. Error bars indicate SD. Data are representative of three independent experiments. *$p < 0.05$, **$p < 0.005$.

by PMA/ionomycin stimulation (Fig. 6A, 6B). Next, we examined whether the binding of NFAT1 and JunB to the IL-31 promoter region was dependent on one another. To address this question we first compared the binding of JunB to the IL-31 promoter in WT CD4$^+$ T cells and NFAT1-deficient CD4$^+$ T cells with or without PMA/ionomycin stimulation. Compared to WT, in NFAT1 KO CD4$^+$ T cells, the binding of JunB to the IL-31 promoter was significantly decreased in only the unstimulated condition (Fig. 6C). We also examined the effect of JunB-dependent NFAT1 binding to the IL-31 promoter by knockdown of JunB expression with siRNA treatment. Binding of NFAT1 to the IL-31 promoter was significantly reduced in JunB siRNA–treated cells as compared with control siRNA–treated cells (Fig. 6D). These results indicate that binding affinity of NFAT1 and JunB to the IL-31 promoter is moderately affected by one aother.

To further confirm the physical binding of NFAT1 to the IL-31 promoter, a DAPA was performed. Three probes for NFAT1 binding sites were designed based on their highest matrix similarity (0.8): NFAT-a (−83/−56), NFAT-b (+91/+120), and NFAT-c (+119/+148) (Fig. 3B). A biotinylated NFAT-a (−83/−56) probe efficiently pulled down NFAT1 protein from NFAT1-transfected HEK-293 cell lysate (*lane 3* in Fig. 7A). Addition of nonbiotinylated competitor probes for NFAT-a (−83/−56), NFAT-b (+91/+120), and NFAT-c (+119/+148) or consensus NFAT probe significantly reduced the pulldown efficiency (*lanes 4–7* in Fig. 7A). However, mutant probes such as mtNFAT-a (−83/−56), mtNFAT-b (+91/+120), mtNFAT-c (+119/+148), and mutated consensus competitor probe failed to inhibit the binding of biotinylated NFAT-a probe (*lanes 8–11* in Fig. 7A). These results confirmed a physical binding of NFAT1 to the IL-31 promoter. We also confirmed the binding of JunB to the predicted JunB binding sites at the IL-31 promoter. The biotinylated AP-1–a (−100/−71) probe effectively pulled down the JunB protein from JunB-transfected HEK-293 cell lysate in a dose-dependent manner (Fig. 7B).

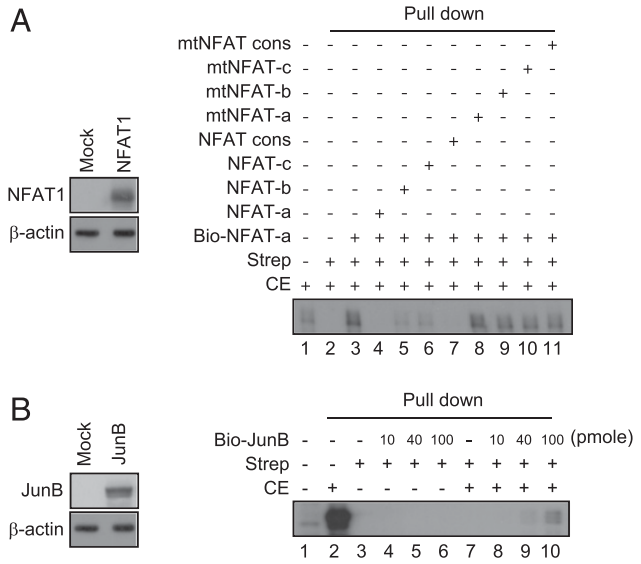


**FIGURE 7.** In vitro binding of NFAT1 and JunB to the *IL-31* promoter locus. (**A** and **B**) *Left*, Controls for overexpression of NFAT1 and JunB in HEK-293 cells and β-actin level (loading control). (A) *Right*, Biotin-conjugated probe corresponding to NFAT-a in Fig. 3B (Bio-NFAT-a) was incubated with cell extract (CE) from NFAT1-overexpressing HEK-293 cells in the presence of indicated WT or mutant nonbiotinylated competitor or NFAT consensus (NFAT cons) probes. The protein–DNA complex was precipitated with streptavidin (Strep) and analyzed by immunoblotting with anti-NFAT1 Ab. (B) *Right*, Indicated amounts of biotin-conjugated probe corresponding to JunB binding site in Fig. 3B (Bio-JunB) was incubated with a lysate from JunB-overexpressing HEK-293 cells. The protein–DNA complex was analyzed by immunoblotting with anti-JunB Ab upon streptavidin-mediated precipitation. (A and B) The *first lane* indicates input control, which is 2.5% of the total CE used for pulldown. Error bars indicate SD. Data are representative of three independent experiments. $*p < 0.05$, $**p < 0.005$.

### *NFAT1 and JunB cooperatively upregulate* IL-31 *gene expression in primary T cells*

To further investigate the functional involvement of NFAT1 and JunB in *IL-31* gene expression, primary CD4$^+$ T cells were transfected with NFAT1 and JunB expression plasmids, and the IL-31 transcript level was measured by qRT-PCR. Transfection of NFAT1 or JunB alone increased IL-31 expression by 6- and 3.2-fold, respectively, compared with control cells (Fig. 8A). Overexpression of both NFAT1 and JunB further increased the IL-31 expression level by 9.8-fold compared with control cells (Fig. 8A). We also tested the knockdown effect of NFAT1 and JunB by siRNA on IL-31 expression. Treatment of siRNA for NFAT1 specifically inhibited the expression of NFAT1 without affecting the expression of other NFAT family members (NFAT2 and NFAT4) (Fig. 8B). Activated CD4$^+$ T cells were transfected with siRNAs for NFAT1 (Fig. 8C), JunB (Fig. 8D), or mock control, and their effects on IL-31 expression were analyzed. Indeed, knockdown of NFAT1 significantly reduced IL-31 mRNA levels (∼40% reduction in Fig. 8E), whereas knockdown of JunB alone failed to do so. Interestingly, however, knockdown of both NFAT1 and JunB significantly reduced IL-31 expression levels (∼80% reduction in Fig. 8E). These results indicate that NFAT1 and JunB cooperatively regulate endogenous IL-31 expression in CD4$^+$ T cells. Next, we also examined the effect of NFAT1 and JunB on the IL-31 expression by the treatment of CsA or tanshinone IIA, inhibitors for calcineurin and AP-1, respectively. Indeed, CsA or tanshinone IIA treatment decreased IL-31 mRNA production by 85 and 40%, respectively. Treatment of both CsA and tanshinone IIA further diminished IL-31 levels by up to 90% (Fig. 8F). To further confirm the pivotal role of NFAT1 in IL-31 expression, we tested the effect of NFAT1 deficiency on IL-31 mRNA level. Compared with CD4$^+$ T cells from WT mice, NFAT1-deficient (N1 KO) CD4$^+$ T cells showed a significant decrease in IL-31 mRNA level upon PMA/ionomycin stimulation (Fig. 8G). We also tested whether reconstitution of NFAT1 into NFAT1-deficient CD4$^+$ T cells could restore the IL-31 expression. NFAT1-expressing plasmid was nucleofected to CD4$^+$ T cells derived from NFAT1 KO mice and after 22 h of nucleofection, and cells were stimulated with PMA/ionomycin for 2 h. Reconstitution efficiency of NFAT1 into NFAT1-deficient CD4$^+$ T cells was confirmed by checking the protein level of NFAT1 by Western blotting (Fig. 8H, *lower panel*). Upon reconstitution of NFAT1 into NFAT1 KO CD4$^+$ T cells, the IL-31 level was partially restored compared with NFAT1 KO CD4$^+$ T cells. Additionally, expression levels of two other well-studied NFAT1 target genes were also partially restored by the reconstitution of NFAT1 to NFAT1 KO CD4$^+$ T cells (Fig. 8H, *right two panels*). These results indicate a crucial role of NFAT1 for IL-31 expression in CD4$^+$ T cells.

### *Essential role of NFAT1 for the IL-31 induction in AD condition*

The IL-31 level is highly increased in AD patients compared with healthy controls (28–30), and treatment with calcineurin inhibitors such as CsA and FK-506 ameliorates atopic symptoms (26). However, the underlying mechanism of increased IL-31 expression in the AD condition is still unclear. To examine the in vivo relevance of NFAT1-mediated *IL-31* gene regulation in the AD condition, we induced experimental AD to ears of BALB/c mice using mite extracts and DNCB. Five weeks after AD induction, CD4$^+$ T cells from normal healthy mice or AD-induced mice were stimulated with PMA/ionomycin or anti-CD3/anti-CD28 for 2 h.

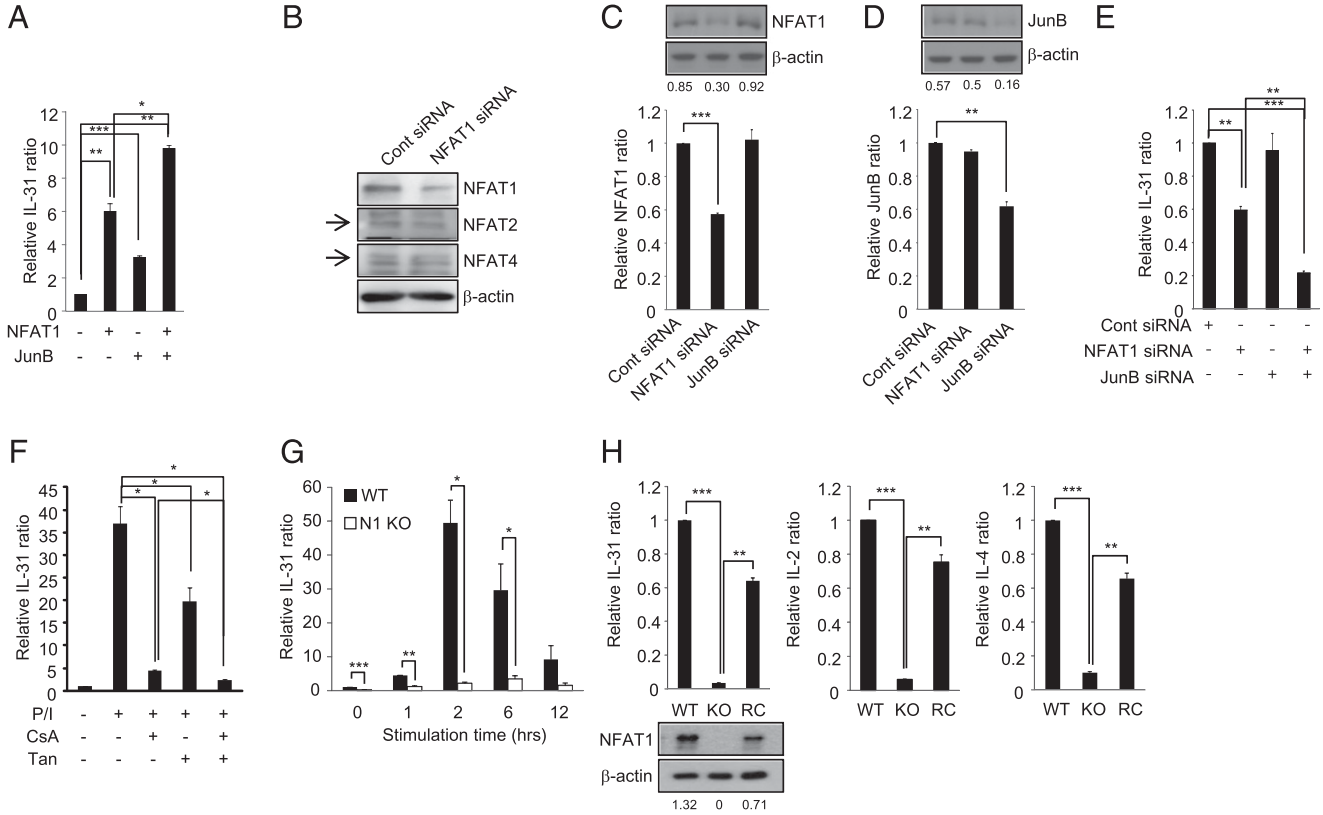


**FIGURE 8.** NFAT1 and JunB mediate endogenous *IL-31* gene expression in CD4$^+$ T cells. (**A**) CD4$^+$ T cells prestimulated with anti-CD3/anti-CD28 for 48 h were nucleofected with expression vectors encoding either NFAT1 or JunB, or in combination. Cells were then stimulated with PMA/ionomycin for 2 h and IL-31 mRNA expression was analyzed by qRT-PCR. (**B**) CD4$^+$ T cells were transfected with siRNA for control or NFAT1, and specificity of NFAT1 knockdown was confirmed by measuring the expression of NFAT2 and NFAT4 by Western blot. Black arrows indicate the specific band for NFAT2 and NFAT4. β-Actin was used as an internal control. (**C** and **D**) CD4$^+$ T cells were transfected with indicated siRNAs and knockdown efficiency and specificity were confirmed by qRT-PCR and Western blot using HPRT and β-actin as the internal loading controls, respectively. Relative density of NFAT1 or JunB band in each sample is shown on the *bottom* of the gel image. C, control siRNA; J, JunB siRNA; N, NFAT1 siRNA. (**E**) CD4$^+$ T cells were transfected with indicated siRNAs and relative IL-31 level was analyzed by qRT-PCR. (**F**) CD4$^+$ T cells were pretreated with CsA, tanshinone IIA (Tan), or both and were stimulated with PMA/ionomycin (P/I) for an additional 2 h. Relative IL-31 level was analyzed by qRT-PCR. (**G**) CD4$^+$ T cells isolated from WT or NFAT1-deficient (N1 KO) mice were stimulated with PMA/ionomycin for indicated time points and subjected to RT-PCR analysis. Mouse HPRT was used as an internal control, and relative IL-31 ratio to WT without stimulation is presented. (**H**) NFAT1 expression was restored by reconstitution of NFAT1encoding plasmid into the NFAT1-deficient (KO) CD4$^+$ T cells, and mRNA expression of IL-31, IL-2, and IL-4 was measured by qRT-PCR. Relative IL-31 ratio to control sample is shown. *Lower panel* demonstrates the reconstitution (RC) efficiency of NFAT1 upon transfection in KO compared with its endogenous level in WT cells. β-Actin was used as an internal control. Error bars indicate SD. Data are representative of three independent experiments. *$p < 0.05$, **$p < 0.005$, **$p < 0.001$.

CD4$^+$ T cells were also stimulated with mite extracts (5 μg/ml) in the presence of T cell–depleted splenocytes as APCs for 24 h. Compared with normal CD4$^+$ T cells, CD4$^+$ T cells from AD-induced mice expressed significantly higher levels of IL-31 mRNA upon PMA/ionomycin or anti-CD3/anti-CD28 stimulation (Fig. 9A, *left panel*) or mite extract (Fig. 9A, *right panel*). Treatment of inhibitors for NFAT1 (CsA) or AP-1 activity (tanshinone IIA) significantly decreased the IL-31 expression compared with the control (Fig. 9B). We found that IL-31–producing NFAT1$^+$ CD4$^+$ T cells were highly increased in the ears of AD-induced mice as compared with healthy mice (Fig. 9C). We found that non–CD4$^+$ T cells also produced much higher amounts of IL-31 under atopic conditions (Supplemental Fig. 2). We tested whether NFAT1 also regulates *IL-31* gene expression in non–CD4$^+$ T cells. Non–CD4$^+$ T cells isolated from WT and NFAT1 KO were stimulated and then relative IL-31 levels were compared. Cells from NFAT1 KO mice showed a significant decrease in the expression level of IL-31 (Supplemental Fig. 3). IL-31 expression was significantly increased in total ear residual cells from-AD induced mice as compared with that of normal mice (Fig. 9D), which was well correlated with increased NFAT1 levels in total cell lysates as well as nuclear extract prepared from total ear cells (Fig. 9E). Increased NFAT1 levels were also found in the cells isolated from the draining lymph nodes and spleen (Supplemental Fig. 4) of AD mice. These results suggest that increased NFAT1 expression in cells mediates the enhanced IL-31 levels in AD condition. We further investigated the functional importance of NFAT1-mediated IL-31 expression in ongoing AD mice. We tested the effect of CsA administration on IL-31 expression under the AD condition. Indeed, oral administration of the microemulsion form of CsA significantly reduced the numbers of IL-31–expressing CD4$^+$ T cells in the AD ears compared with those of control mice (Fig. 9F). Treatment of CsA significantly decreased the expression of IL-31 as well as AD-related pathogenic cytokines such as IL-4, IL-13, and IFN-γ in the ear total cells (Fig. 9G). This result indicates that inhibition of NFAT1 activity suppressed AD development by reducing the IL-31 expression by CD4$^+$ T cells and non–CD4$^+$ T cells as well.

## Discussion

The main purpose of this study was to elucidate the molecular mechanism of *IL-31* gene regulation in CD4$^+$ T cells in health and disease. We identified the TSS and functional promoter region of *IL-31* gene. We found that TCR-induced IL-31 expression is mediated by a functional cooperation between two transcription factors,

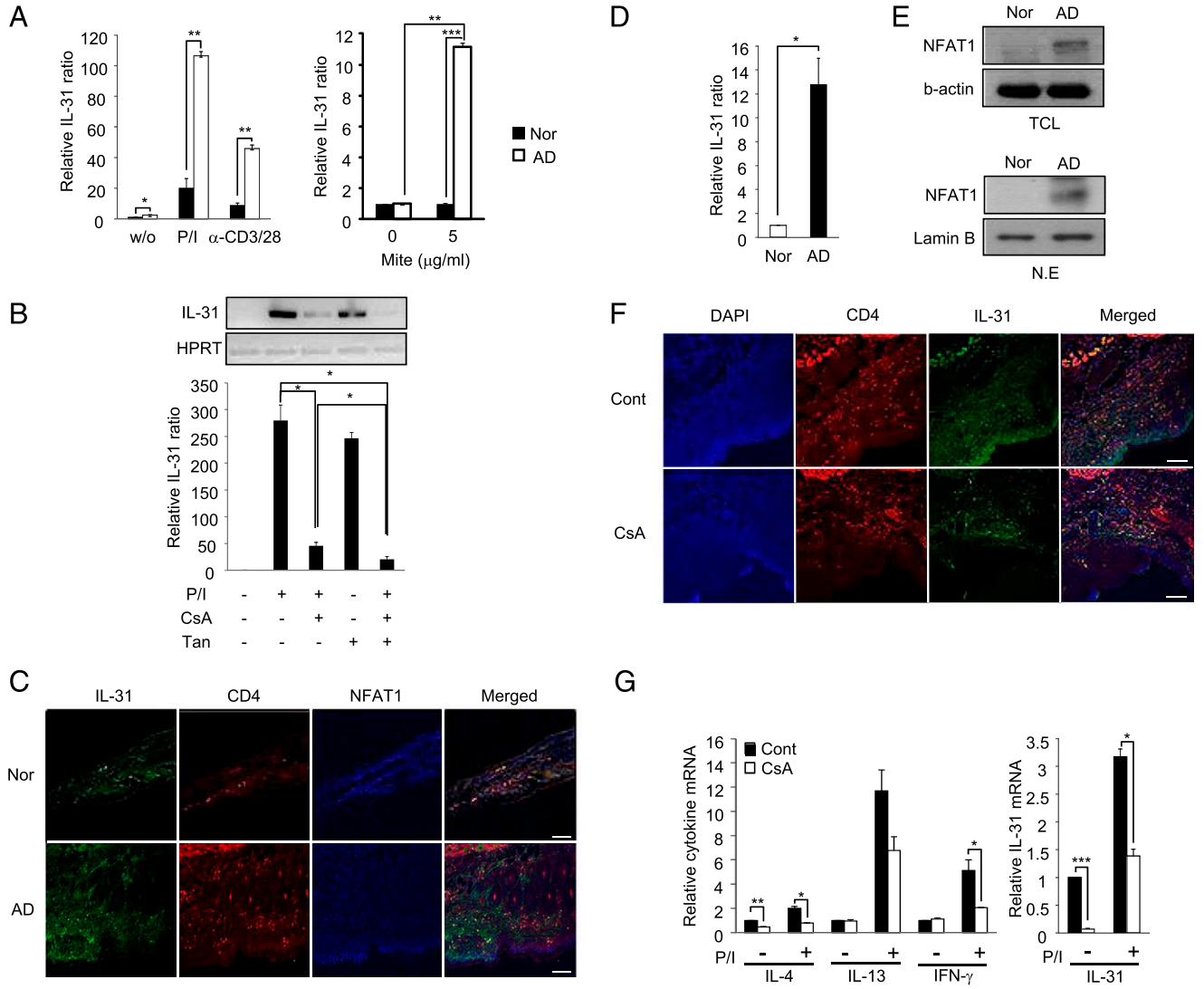


**FIGURE 9.** NFAT1 mediates enhanced IL-31 expression in AD. (**A**) Isolated CD4$^+$ T cells from normal (Nor) and atopic mice (AD) were untreated (w/o) or stimulated with anti-CD3/anti-CD28, PMA/ionomycin (P/I) (*left*), or mite extract (*right*). Relative level of IL-31 expression was analyzed by qRT-PCR, and relative IL-31 ratio to normal mice without AD (Nor) sample is presented. (**B**) CD4$^+$ T cells isolated from AD-induced mice were pretreated with indicated inhibitors for NFAT (CsA) or AP-1 (tanshinone IIA [Tan]) and their effect on IL-31 expression was measured by qRT-PCR (*bottom*) and visualized in agarose gel (*top*). (**C**) Triple immunohistochemical staining was performed on ear sections from normal (Nor) and AD-induced mice with Abs against NFAT1 (blue), IL-31(green), and CD4 (red). Scale bars, 100 μm. (**D**) Relative IL-31 expression was analyzed in total ear cells from normal (Nor) and AD-induced mice by qRT-PCR. (**E**) Protein expression level of NFAT1 in total cell lysates (TCL) and nuclear extract (N.E) of total ear cells from normal (Nor) and AD-induced mice was measured by Western blot. β-Actin and lamin B were used as a loading control. (**F**) Microemulsion form of CsA (5 mg/kg/d) was orally administrated to atopic mice. Immunohistochemical staining was performed on the ear sections of control (Cont; DMSO) and CsA-treated (CsA) mice with anti-CD4 Ab (red) and anti–IL-31 Ab (green) and counterstained with DAPI (blue) for nuclei. Scale bars, 100 μm. (**G**) Total cells isolated from ears of control (Cont) or CsA-treated (CsA) mice were either unstimulated (−) or stimulated (+) with PMA/ionomycin (P/I) for 2 h. Indicated cytokine levels were analyzed by qRT-PCR. Relative expression of each cytokine was analyzed by comparing with the value of unstimulated (−) control (Cont) samples. Error bars indicate SD. Data are representative of three independent experiments. $*p < 0.05$, $**p < 0.005$, $***p < 0.001$.

NFAT1 and JunB (AP-1). Physical binding of NFAT1 and JunB to the IL-31 promoter region increased its transcriptional activity. Under atopic conditions, enhanced infiltration of NFAT1$^+$CD4$^+$ T cells on the AD ears was well correlated with a significant increase of IL-31 expression. Treatment of inhibitors for NFAT1 and JunB (AP-1) significantly decreased IL-31 expression in CD4$^+$ T cells of AD mice. Our results suggest that NFAT1 and JunB cooperatively regulate the IL-31 transcription in CD4$^+$ T cells in both normal and AD conditions.

Functional importance of IL-31 in diverse immune disorders has been suggested (27–31). However, the underlying mechanism of IL-31 expression at the transcriptional levels is still unclear. In this study, we have identified the TSS (Fig. 2C) and functional promoter region, located between the region −359 and +141 of the *IL-31* gene (Fig. 3C). A previous study on human IL-31 reported a functional promoter region in CD4$^+$ T cells and mast cells (32) without revealing an exact TSS. We compared human and mouse promoter regions and transcription factors responsible for the activation of promoters (Supplemental Fig. 1A). The human IL-31 promoter (827 bp) contains conserved binding sites for several transcription factors such as NFAT, STAT6, AP-1 and NF-κB. Among the factors, NFAT2 and STAT6 played a major role in activation of its promoter activity (32). We also tested whether NFAT2 and STAT6 could activate mouse IL-31 promoter as well. However, NFAT2 and STAT6 failed to activate mouse IL-31 promoter whereas NFAT1 alone sufficiently activated the mouse

IL-31 promoter in a STAT6-independent manner (Supplemental Fig. 1B). Interestingly, the STAT6 binding site identified in the human IL-31 promoter was matched with NFAT binding sites of the mouse IL-31 promoter (Supplemental Fig. 1A). This finding suggests that NFAT may play a crucial role in regulation of IL-31 expression both in humans and mice although different NFAT family members are responsible for activation of the IL-31 promoter. Indeed, NFAT2 and NFAT4 also showed transactivity on mouse IL-31 promoter, although NFAT1 showed the strongest activity (Fig. 4A). Functional synergism between NFAT/AP-1 interaction has been reported in regulation of diverse NFAT target genes such as IL-2, IL-4, IL-5, IL-13, and INF-γ (18, 33, 34). In this study we also found that whereas NFAT1 alone significantly unregulated IL-31 promoter activity, AP-1 binding had a positive contribution (Fig. 4C). Deleting (Fig. 4E) or mutating (Fig. 4F) NFAT or AP-1 binding sites or treating them with their inhibitors (Fig. 8F) significantly reduced IL-31 promoter activity as well as IL-31 mRNA expression. Additionally, disruption of physical interaction between NFAT1 and AP-1 abolished the synergistic transactivity on the IL-31 promoter (Fig. 4D). These results collectively suggest a functional synergism of NFAT1/AP-1 interaction in *IL-31* gene regulation.

Pathophysiological role of IL-31 has been reported in diverse immune disorders, including AD (32–35). Compared with normal healthy people, a significant increase in IL-31 levels was observed in AD patients along with the upregulation of IL-4 and IL-13 (29). Enhanced IL-31 levels from Th2 cells activated IL-31RA–expressing neurons, which induced a T cell–mediated itching behavior (29, 36). Additionally, IL-31 induces the upregulation of AD-associated pathogenic cytokines (TNF-α, IL-6, and IL-1β) and chemokines (CXCL8, CCL2, CCL5, CXCL1, CCL18, and CCL22) by dendritic cells, macrophages, epithelial cells, eosinophils, and keratinocytes (4, 37, 38). In this study, we also found that $CD4^+$ T cells isolated from AD mice showed a significant increase of IL-31 expression upon TCR- or allergen (mite extract)–specific stimulation (Fig. 9) mainly in draining lymphocytes (Supplemental Fig. 4). Immunostaining of IL-31 on sections of AD ear showed that although $CD4^+$ T cells are the main source of IL-31, non–$CD4^+$ cells also produce large amount of IL-31 as well (Fig. 9C, Supplemental Fig. 2B). We also found that non–$CD4^+$ T cells from NFAT1 KO mice showed a significant decrease in IL-31 mRNA expression as compared with normal mice (Supplemental Fig. 3). These results imply that NFAT1 plays a crucial role for *IL-31* gene expression in both $CD4^+$ T cells and non–$CD4^+$ T cells. However further studies are required to identify which kind of NFAT proteins play a key role in regulation of IL-31 expression in non–$CD4^+$ T cells. Interestingly, severity of AD symptoms was well correlated with $NFAT1^+$ signal and IL-31 expression both in $CD4^+$ T cells and in non–$CD4^+$ T cells. CsA, an inhibitor of $Ca^{2+}$/calmodulin/calcineurin/NFAT signaling had been used to treat AD symptoms (36). CsA treatment decreases the severity of AD in patients by inhibiting the production of several cytokines from T cells (37, 38). In this study we found that the beneficial effect of CsA treatment on AD suppression could be explained by an inhibition of NFAT1-mediated IL-31 expression in both $CD4^+$ T cells and non–$CD4^+$ T cells (Fig. 9F, 9G).

In summary, we demonstrated the NFAT1 plays a key role in regulate of *IL-31* gene expression in $CD4^+$ T cells and non–$CD4^+$ T cells in normal and disease conditions. Recruitment of JunB as a cofactor for activation of the IL-31 promoter further activated NFAT1-mediated IL-31 expression. Our results suggest that the beneficial effect of CsA for AD treatment can be explained by inhibition of NFAT-mediated IL-31 expression in both $CD4^+$ T cells and non–$CD4^+$ T cells.

## Acknowledgments

We thank our colleagues in the laboratory for valuable comments on this work.

## Disclosures

The authors have no financial conflicts of interest.

## References

1. Cornelissen, C., R. Brans, K. Czaja, C. Skazik, Y. Marquardt, G. Zwadlo-Klarwasser, A. Kim, D. R. Bickers, J. Lüscher-Firzlaff, B. Lüscher, and J. M. Baron. 2011. Ultraviolet B radiation and reactive oxygen species modulate interleukin-31 expression in T lymphocytes, monocytes and dendritic cells. *Br. J. Dermatol.* 165: 966–975.
2. Dillon, S. R., C. Sprecher, A. Hammond, J. Bilsborough, M. Rosenfeld-Franklin, S. R. Presnell, H. S. Haugen, M. Maurer, B. Harder, J. Johnston, et al. 2004. Interleukin 31, a cytokine produced by activated T cells, induces dermatitis in mice. *Nat. Immunol.* 5: 752–760.
3. Le Saux, S., F. Rousseau, F. Barbier, E. Ravon, L. Grimaud, Y. Danger, J. Froger, S. Chevalier, and H. Gascan. 2010. Molecular dissection of human interleukin-31-mediated signal transduction through site-directed mutagenesis. *J. Biol. Chem.* 285: 3470–3477.
4. Kasraie, S., M. Niebuhr, and T. Werfel. 2013. Interleukin (IL)-31 activates signal transducer and activator of transcription (STAT)-1, STAT-5 and extracellular signal-regulated kinase 1/2 and down-regulates IL-12p40 production in activated human macrophages. *Allergy* 68: 739–747.
5. Dambacher, J., F. Beigel, J. Seiderer, D. Haller, B. Göke, C. J. Auernhammer, and S. Brand. 2007. Interleukin 31 mediates MAP kinase and STAT1/3 activation in intestinal epithelial cells and its expression is upregulated in inflammatory bowel disease. *Gut* 56: 1257–1265.
6. Broxmeyer, H. E., J. Li, G. Hangoc, S. Cooper, W. Tao, C. Mantel, B. Graham-Evans, N. Ghilardi, and F. J. de Sauvage. 2007. Regulation of myeloid progenitor cell proliferation/survival by IL-31 receptor and IL-31. *Exp. Hematol.* 35(4, Suppl. 1)78–86.
7. Stott, B., P. Lavender, S. Lehmann, D. Pennino, S. Durham, and C. B. Schmidt-Weber. 2013. Human IL-31 is induced by IL-4 and promotes $T_H2$-driven inflammation. *J. Allergy Clin. Immunol.* 132: 446–454.e5.
8. Ip, W. K., C. K. Wong, M. L. Y. Li, P. W. Li, P. F. Y. Cheung, and C. W. K. Lam. 2007. Interleukin-31 induces cytokine and chemokine production from human bronchial epithelial cells through activation of mitogen-activated protein kinase signalling pathways: implications for the allergic response. *Immunology* 122: 532–541.
9. Baumann, R., M. Rabaszowski, I. Stenin, M. Gaertner-Akerboom, K. Scheckenbach, J. Wiltfang, J. Schipper, and M. Wagenmann. 2012. The release of IL-31 and IL-13 after nasal allergen challenge and their relation to nasal symptoms. *Clin Transl Allergy* 2: 13.
10. Zhang, Q., P. Putheti, Q. Zhou, Q. Liu, and W. Gao. 2008. Structures and biological functions of IL-31 and IL-31 receptors. *Cytokine Growth Factor Rev.* 19: 347–356.
11. Ezzat, M. H. M., Z. E. Hasan, and K. Y. A. Shaheen. 2011. Serum measurement of interleukin-31 (IL-31) in paediatric atopic dermatitis: elevated levels correlate with severity scoring. *J. Eur. Acad. Dermatol. Venereol.* 25: 334–339.
12. Neis, M. M., B. Peters, A. Dreuw, J. Wenzel, T. Bieber, C. Mauch, T. Krieg, S. Stanzel, P. C. Heinrich, H. F. Merk, et al. 2006. Enhanced expression levels of IL-31 correlate with IL-4 and IL-13 in atopic and allergic contact dermatitis. *J. Allergy Clin. Immunol.* 118: 930–937.
13. Sonkoly, E., A. Muller, A. I. Lauerma, A. Pivarcsi, H. Soto, L. Kemeny, H. Alenius, M.-C. Dieu-Nosjean, S. Meller, J. Rieker, et al. 2006. IL-31: a new link between T cells and pruritus in atopic skin inflammation. *J. Allergy Clin. Immunol.* 117: 411–417.
14. Bilsborough, J., D. Y. M. Leung, M. Maurer, M. Howell, M. Boguniewicz, L. Yao, H. Storey, C. LeCiel, B. Harder, and J. A. Gross. 2006. IL-31 is associated with cutaneous lymphocyte antigen-positive skin homing T cells in patients with atopic dermatitis. *J. Allergy Clin. Immunol.* 117: 418–425.
15. Bando, T., Y. Morikawa, T. Komori, and E. Senba. 2006. Complete overlap of interleukin-31 receptor A and oncostatin M receptor β in the adult dorsal root ganglia with distinct developmental expression patterns. *Neuroscience* 142: 1263–1271.
16. Takaoka, A., I. Arai, M. Sugimoto, A. Yamaguchi, M. Tanaka, and S. Nakaike. 2005. Expression of IL-31 gene transcripts in NC/Nga mice with atopic dermatitis. *Eur. J. Pharmacol.* 516: 180–181.
17. Macian, F. 2005. NFAT proteins: key regulators of T-cell development and function. *Nat. Rev. Immunol.* 5: 472–484.
18. Müller, M. R., and A. Rao. 2010. NFAT, immunity and cancer: a transcription factor comes of age. *Nat. Rev. Immunol.* 10: 645–656.
19. Crabtree, G. R., and E. N. Olson. 2002. NFAT signaling: choreographing the social lives of cells. *Cell* 109(Suppl.): S67–S79.
20. Rao, A., C. Luo, and P. G. Hogan. 1997. Transcription factors of the NFAT family: regulation and function. *Annu. Rev. Immunol.* 15: 707–747.
21. Fric, J., T. Zelante, A. Y. W. Wong, A. Mertes, H.-B. Yu, and P. Ricciardi-Castagnoli. 2012. NFAT control of innate immunity. *Blood* 120: 1380–1389.
22. Sahoo, A., C.-G. Lee, A. Jash, J.-S. Son, G. Kim, H.-K. Kwon, J.-S. So, and S.-H. Im. 2011. Stat6 and c-Jun mediate Th2 cell-specific IL-24 gene expression. *J. Immunol.* 186: 4098–4109.
23. Kwon, H.-K., C.-G. Lee, J.-S. So, C.-S. Chae, J.-S. Hwang, A. Sahoo, J. H. Nam, J. H. Rhee, K.-C. Hwang, and S.-H. Im. 2010. Generation of regulatory dendritic cells and $CD4^+Foxp3^+$ T cells by probiotics administration suppresses immune disorders. *Proc. Natl. Acad. Sci. USA* 107: 2159–2164.

24. Park, K., J.-H. Park, W.-J. Yang, J.-J. Lee, M.-J. Song, and H.-P. Kim. 2012. Transcriptional activation of the *IL31* gene by NFAT and STAT6. *J. Leukoc. Biol.* 91: 245–257.
25. Macián, F., C. García-Rodríguez, and A. Rao. 2000. Gene expression elicited by NFAT in the presence or absence of cooperative recruitment of Fos and Jun. *EMBO J.* 19: 4783–4795.
26. Alaiti, S., S. Kang, V. C. Fiedler, C. N. Ellis, D. V. Spurlin, D. Fader, G. Ulyanov, S. D. Gadgil, A. Tanase, I. Lawrence, et al. 1998. Tacrolimus (FK506) ointment for atopic dermatitis: a phase I study in adults and children. *J. Am. Acad. Dermatol.* 38: 69–76.
27. Rabenhorst, A., and K. Hartmann. 2014. Interleukin-31: a novel diagnostic marker of allergic diseases. *Curr. Allergy Asthma Rep.* 14: 423.
28. Shah, S. A., H. Ishinaga, B. Hou, M. Okano, and K. Takeuchi. 2013. Effects of interleukin-31 on MUC5AC gene expression in nasal allergic inflammation. *Pharmacology* 91: 158–164.
29. Yu, J.-I., W.-C. Han, K.-J. Yun, H.-B. Moon, G.-J. Oh, and S.-C. Chae. 2012. Identifying polymorphisms in IL-31 and their association with susceptibility to asthma. *Korean J. Pathol.* 46: 162–168.
30. Lee, C. H., C. H. Hong, W. T. Yu, H. Y. Chuang, S. K. Huang, G. S. Chen, T. Yoshioka, M. Sakata, W. T. Liao, Y. C. Ko, and H. S. Yu. 2012. Mechanistic correlations between two itch biomarkers, cytokine interleukin-31 and neuropeptide β-endorphin, via STAT3/calcium axis in atopic dermatitis. *Br. J. Dermatol.* 167: 794–803.
31. Ouyang, H., J. Cheng, Y. Zheng, and J. Du. 2014. Role of IL-31 in regulation of Th2 cytokine levels in patients with nasal polyps. *Eur. Arch. Otorhinolaryngol.* 271: 2703–2709.
32. Szegedi, K., A. E. Kremer, S. Kezic, M. B. M. Teunissen, J. D. Bos, R. M. Luiten, P. C. Res, and M. A. Middelkamp-Hup. 2012. Increased frequencies of IL-31-producing T cells are found in chronic atopic dermatitis skin. *Exp. Dermatol.* 21: 431–436.
33. Wong, C.-K., K. M.-L. Leung, H.-N. Qiu, J. Y.-S. Chow, A. O. K. Choi, and C. W.-K. Lam. 2012. Activation of eosinophils interacting with dermal fibroblasts by pruritogenic cytokine IL-31 and alarmin IL-33: implications in atopic dermatitis. *PLoS ONE* 7: e29815.
34. Henderson, P., J. E. van Limbergen, J. Schwarze, and D. C. Wilson. 2011. Function of the intestinal epithelium and its dysregulation in inflammatory bowel disease. *Inflamm. Bowel Dis.* 17: 382–395.
35. Ständer, S., U. Raap, E. Weisshaar, M. Schmelz, T. Mettang, H. Handwerker, and T. A. Luger. 2011. Pathogenesis of pruritus. *J. Dtsch. Dermatol. Ges.* 9: 456–463.
36. Cevikbas, F., X. Wang, T. Akiyama, C. Kempkes, T. Savinko, A. Antal, G. Kukova, T. Buhl, A. Ikoma, J. Buddenkotte, et al. 2014. A sensory neuron-expressed IL-31 receptor mediates T helper cell-dependent itch: Involvement of TRPV1 and TRPA1. *J. Allergy Clin. Immunol.* 133: 448–460, e447.
37. Horejs-Hoeck, J., H. Schwarz, S. Lamprecht, E. Maier, S. Hainzl, M. Schmittner, G. Posselt, A. Stoecklinger, T. Hawranek, and A. Duschl. 2012. Dendritic cells activated by IFN-γ/STAT1 express IL-31 receptor and release proinflammatory mediators upon IL-31 treatment. *J. Immunol.* 188: 5319–5326.
38. Cheung, P. F.-Y., C.-K. Wong, A. W.-Y. Ho, S. Hu, D.-P. Chen, and C. W.-K. Lam. 2010. Activation of human eosinophils and epidermal keratinocytes by Th2 cytokine IL-31: implication for the immunopathogenesis of atopic dermatitis. *Int. Immunol.* 22: 453–467.